f

MUC/NOTE/COOL-EXP//216

Preliminary design of the magnets for the double flip cooling channel.

V.Balbekov, E.Black, C. Darve, D. Elvira, J.M.Rey.

1 – Introduction.

This report proposes a design of the magnets for the double flip cooling channel for the neutrino factory, as proposed in the reference design made by V. Balbekov [(1)]. The magnet design is based on reliable technologies and makes the benefits of recent developments made for large detector magnets. The proposal is also made to identify R&D developments needed to make a large solenoid based machine.

2 – Presentation of the two flips cooling channel and general design layout.

2.1 – Magnetic requirements.

The double flip cooling channel design is based on constant magnetic field over long length and the magnets should be as near as possible to the infinite solenoids. Therefore efforts should be made to limit the areas without conductors, and reduce the field variation along the axis in the constant field zones.
The successive sections of the cooling channel are the following:

- Constant field of 3T over 48.4 m.
- Flip change 3T to –3T over 1.02 m.
- Continuous field changes from –3T to –7T over 53.22 m.
- Constant field of -7T over 75.1 m.
- Flip change -7T to 7T over 1.26 m.
- Constant field of 7T over 37.54 m.

2.2 – Space requirements.

The length of the accelerating cavities and their respective liquid hydrogen absorbers defines the length and the inner bore diameter of the magnets. The length of the magnet is 2.31 m in the low field region and 2.4 m in the high field region and the inner bore radius is 0.8 m. The accelerating cavities and the liquid hydrogen absorbers need their own supply which are located every two magnets. The distance between two magnets is 200 mm where the electrical and cryogenic supplies are located and 20 mm at their other end. These space constrain, and the need to have a field almost homogeneous over long length have leaded to a magnet design where the compaction of the winding is not the same over the entire length of the magnets.

2.3 - Coils design and manufacturing technique.

2.3.1 – Conductor.

The conductors of each of the magnets are stabilized with nickel reinforced aluminum[3]. The quantity of superconducting material and of aluminum stabilizer is adapted for each layer. This technique allows saving superconducting material in the layer producing a low field and to ensure a good stability margin on the conductor operating under a high background field. The number of superconducting strands is adapted for each winding layer in the coils. The cable used in the innermost conductor has more superconducting strands than the outer ones. The cables used for the outer layers include copper strands which contribute to the quench protection by reducing the resistance of the conductor during the transient time of current diffusion in the stabilizer. The cross section of aluminum stabilizer is also adapted for each winding layer. The innermost conductors, where the field is the highest, and where the superconducting material has the lower stability margin, have more stabilizer than the other layers. The complementary copper strands on the outer layers and the larger quantity of aluminum in the inner layer also helps spreading the magnetic force over the whole thickness of the magnet.

2.3.2 – Mechanical structure.

Aluminum alloys tubes provide the mechanical structure. Each layer of conductor is winded inside of one tube that carries the magnetic forces when the magnet is energized. The tube thickness is adapted to reduce the load transfer from one conductor layer to the other.

2.3.3 - Cooling mode.

The magnets are cooled by conduction. The liquid helium used as coolant flows in aluminum tubes glued on the external tube supporting the winding. To limit the effect of the heat deposition coming from the particle beam and the RF cavities, a 1 mm thick pure aluminum foil is placed in the inner bore of the magnet. This aluminum foil is cooled by its own cooling tube and acts as a thermal drain.

2.3.4 – Insulation.

The insulation is made of glass fiber ribbons impregnated with epoxy resin. The glass fiber ribbons are wrapped around the conductor during the winding process, the impregnation takes place at the end of the winding operation. The impregnation of epoxy resin is a very common technique[4,5,6,7] used in the industry. The coil is kept under vacuum and slowly filled with liquid epoxy resin. The resin is then cured to reach a solid state. This technique ensures the mechanical and thermal continuity of the coils, both properties of main importance in the case of conduction cooled magnets.

The thickness of the insulation is also adjusted to provide some variation in the current density along the solenoid. This allows shaping the field on the solenoid axis to limit the negative effects of the gaps. The adjustment can be made by changing the thickness of the fiber ribbons or by inserting composite shims or aluminum spacers between turns.

2.3.5 – Winding technique.

The coils are wound using an internal winding technique[4]. The conductor is first preformed to the convenient radius using a turkhead and then inserted in the tube acting as an external mandrel. The bending radius imposed by the turkhead is slightly greater than the inner radius of the mandrel. The conductor is kept under elastic strain that pushes him on the mandrel. The mandrel also supports most of the forces during operation. Considering the large level of forces due to the magnetic field, each layer of conductor has a supporting tube.

2.3.6 – Quench protection.

Once a quench is detected in one magnet, the whole magnet is driven in the resistive state as fast as possible. This is done by quench propagation heaters placed at each end of each layer. The quantity of stabilizer is greater in the conductor seeing the highest field, where a quench is most likely to occur, than in the other conductors. Therefore the high field conductor will heat up slowly compared to the other

conductors, thus letting time to start the quench heaters and to propagate the quench in the whole coil. Once the quench is propagated to all the layers, the resistivity of the magnet increases rapidly. As the resistivity increases the main current is by passed from the quenched coil in a diode.
The protection in case of a transition to the superconducting state is helped by the quench back effect. During the decay of the current in the winding, the supporting structure acts as a transformer. The current generated in the structure heats it by Joule effect. Nevertheless since the supporting structure is thick, the current density induced by the current decay in the winding, and then the heating, are low.
The quench in one magnet will induce a quench in its neighbors after a short delay.

2.4 – Electrical circuit.

The electrical circuit comprises several magnets in serie. The nominal current has been limited to around 20 kA for electrotechnical reasons (increase of the cost of the power supply, the current leads and the electrical buses).
The current used to energize the magnets is high (19760 A) in order to limit the inductance of the magnets, and to reduce the dump time of each magnet in the case of a quench. All the magnets are powered with the same current. This limits the number of conductors to be developed and limits the cost.

2.5 - Coil and cryostat identification.

The assembly of the complete channel is made by sub-elements. Each of the sub elements comprises one cryostat, two main magnets two accelerating cavities and two absorbers. The sub elements have to be removable from the beam line separately. The cryostats are numbered from 1 to 46. The coils are designated A, B and C in all the sub elements except the two flips region, A and B representing the main coils and C the compensation coil put inside the 200 mm gap. In the flip regions the coils are numbered A, B, C and D, A and B for the outer coils, C and D for the inner ones. The coil designation comes after the number referring to the cryostat. A complete list of the coils and cryostat is presented in appendix 1.

3 – Uniform field zones.

3.1 – Stored energy and magnetic pressure.

The stored energy and the magnetic pressure for the low field and high field magnets are presented in table 3-1.

	Magnetic Field T	Stored Energy MJ	Magnetic Pressure MPa
Low field coil	3	18.2	3.7
High field coil	7	128	21.2

Table 3-1: on axis magnetic field, stored energy and magnetic pressure of the solenoids.

3.2 – Conductor design.

3.2.1 - Strand choice.

The main characteristics of the strands are typical of standard production so as to minimize the cost and to ensure the best reliability:

- The filament diameter is in the range of 50 μm, convenient for steady field magnets.
- The Cu/SC ratio can be chosen between 1.1 to 1.4 to ease the wire drawing fabrication and limit the cabling degradation.
- The strand diameter is between 1.2 and 1.4mm. These values are compatible with the number of strands required for the different conductors.

Retained strands characteristics are summarized in table 3-2.

Strand diameter	mm	1.4
Copper to SC ratio		1.1
Critical current	@ 5T & 4.2K	2180 A
Critical temperature	@ 5T	6.58 K
Section of NbTi	mm^2	0.73
Section of Copper	mm^2	0.81

Table 3-2: superconducting strands characteristics.

3.2.2 – Low field magnets.

The low field magnets (i.e. the magnets generating the 3T homogeneous field) are realized using one layer of conductor. The mean current density per unit length varies from 2430 A/mm to 2470 A/mm.
Considering the supply power of 19760 A, the conductor thickness is 7.2 mm, with a 0.8 mm interturn insulation in the high density zone. In the low density zone the insulation thickness increases to 0.93 mm. The total number of turns is 285, giving an inductance of 87 mH per solenoid.

3.2.3 – High field magnets.

The magnets generating the 7T field are realized using 3 layers of conductor carrying a mean current density of 5815 A per mm of length. The conductor on the external layer is the same than the one used for the low field magnets. The two other layers produce respectively 2.3T and 1.7T for the middle and inner layer.

Considering the supply power of 19760 A, the conductors thickness are 8.83 mm and 11.93 mm respectively for the middle and inner layer. A 0.8 mm interturn insulation is used in the high density zone. For the low density zone the interturn insulation thickness increases to 1.56 mm in the middle layer, and to 2.18 mm in the inner layer. The total number of turns is 706, giving an inductance of 503 mH per solenoid.

		Low field and outer layer conductor	High field middle layer conductor	High field inner layer conductor
Conductor thickness	mm	7.2	8.83	11.93
Conductor width	mm	35	35	35
Number of SC strands		12	18	32
Number of copper strands		18	18	
Critical current	@ 4.2K & 5T	26 400 A	39 570 A	70 380 A
Section of Stabilizer	mm^2	279	360	444

Table 3-3: characteristics of the different conductors.

Copper strands are added to the cable for the low field and middle layer conductors. They are used to improve the protection of the coil in the case of a quench. The influence of the copper strands will be discussed in section 3.4.3.

3.2.3 – Operating point and stability margin.

The limiting factor for the NbTi superconducting material are strongly dependant on the magnetic field and temperature[8]. The operating point for each conductor is defined as the ratio of the operating current density to the critical current density for the maximum field seen by each of the layers. The stability margin is defined as the temperature rise needed to reduce the critical current density down to the operating current density on each of the layers. Figure 3-1 shows the operating points of the different layers of the 7T magnets. The data are summarized for each of the conductors on table 3-4.

The peak field on the low field conductor being 3T, the critical current under this field is 4510 A/mm^2. Using a cable made of 12 strands of 1.4 mm in diameter and having a copper to superconductor ratio of 1.1 the operating point is 0.5.

The peak field on the two other conductors for the high field magnets being 5.3T and 7T for respectively the middle and inner layer, the critical current under these fields are respectively 2790 A/mm^2 and 1770 A/mm^2. Using cables made of the same strands than the low field conductor, 18 strands are required on the middle layer and 32 strands on the inner layer. The operating points are respectively 0.54 and 0.48.

		Low field and outer layer conductor	High field middle layer conductor	High field inner layer conductor
Operating field	T	3	5.3	7
Critical current	@ 4.2K & op.field	39 680 A	36 820 A	41 450 A
Critical current density	@ 4.2K & op.field	4511	2791	1767
Operating point		0.50	0.54	0.48
Critical temperature	K	7.39	6.46	5.7
Thermal stability margin	K	2.89	1.96	1.2
Current sharing temperature	K	5.95	5.4	5.13

Table 3-4: Operating points and stability margin for each of the superconducting cables.

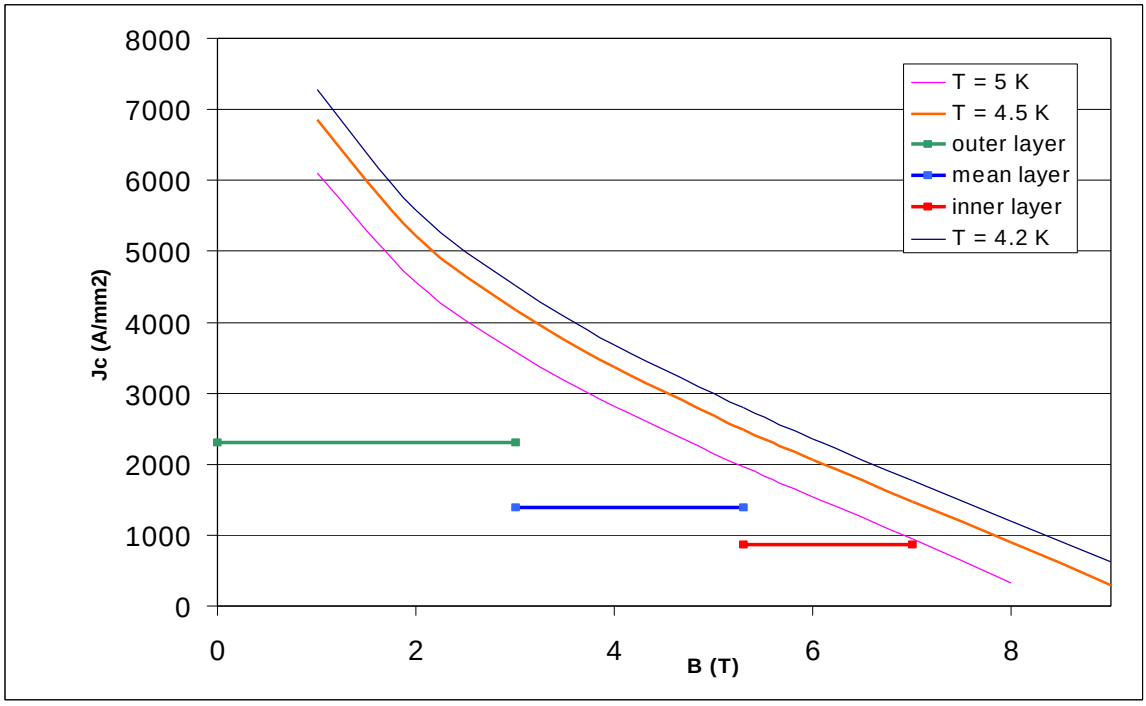

Figure 3-1: critical current density of NbTi superconductor as a function of magnetic field. The short lines represent the places of the conductors used respectively for the outer, mean and inner layer of the high field magnets.

3.3 – Mechanical structure.

3.3.1 – Low field magnets.

The low field magnets have to withstand a magnetic pressure of 3.6 MPa, creating a hoop stress of 84 MPa in the winding. To withstand the hoop stress, an external cylinder of aluminum alloy is used. Its thickness is 25 mm.

This external cylinder is also used as an external mandrel for the winding (detailed in section 8-1).

Including this external cylinder the mean hoop stress in the magnet comes down to 55 MPa.

3.3.2 – High field magnets.

The high field magnets have to withstand a magnetic pressure of 21.2 MPa. This magnetic pressure would create a hoop stress of 160 MPa, far above what can be supported by the aluminum reinforced conductor[(3)]. Three aluminum alloy cylinders are added, one external and one between each layer of conductor. Their respective thickness are 13 mm, 35 mm and 35 mm. The mean hoop stress in the magnet comes down to 96 MPa. The intermediate cylinders are determined in order to keep the mean stress of each of the set of winded layer and supporting cylinder at a stress level around 100 MPa. The different stresses on each of the layers and supporting structure are summarized in table 3-5. The estimated mass of the different coils is also presented.

		Low field magnet	High field magnet
Mean hoop stress	MPa	54.4	96.4
External mandrel thickness	mm	25	13
Hoop stress on the external layer and external mandrel	MPa	54.4	79.6
Intermediate mandrel thickness	mm		35
Hoop stress on the middle layer and intermediate mandrel	MPa		102.5
Inner mandrel thickness	mm		35
Hoop stress on the inner layer and inner mandrel	MPa		101.8
Mass of the winding and supporting structure	kg	1950	6850

Table 3-5: Mean stress on the different sub-elements of the structure of the high field magnets.

3.4 – Field homogeneity.

3.4.1 – Low field magnets.

The field produced by the low field magnets varies along the coil axis from 3.1T to 2.95T with the coil compensation or from 2.98T to 2.69T without. The main coils consists of 1.7 m length having a current density of 2430A per mm length and 0.61 m having a current density of 2470 A/mm. The two length of 0.61 m are placed on each side of the 200 mm gap. Inside the gap a 200 mm a compensation coil (described in 3.4.3) may be placed to limit the field degradation due to the gap.

Figure 3-2 shows the field along the solenoid axis with and without compensation coil.

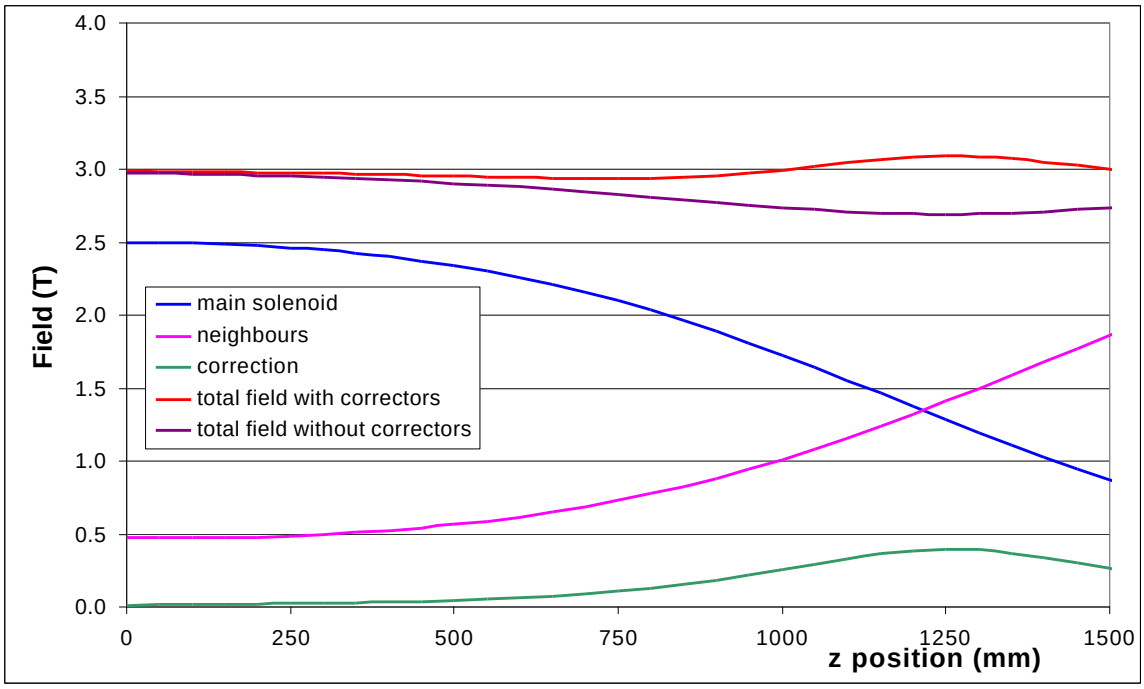

Figure 3-2: on axis low field with and without corrector coils.

3.4.2 – High field magnets.

Considering the conductors presented in 3.2 and the mechanical structure presented in 3.3, the field varies along the coil axis from 6.87T to 7T with the coil compensation or from 6.54T to 6.99T without. The main coils consists of 1.8 m length having a current density of 5730A per mm length and 0.6 m having a current density of 6070 A/mm. The two length of 0.6 m are placed on each side of the 200 mm gap. Inside the gap a 200 mm a compensation coil (described in 3.4.3) may be placed to limit the field degradation due to the gap. Figure 3-3 shows the field along the solenoid axis with and without compensation coil.

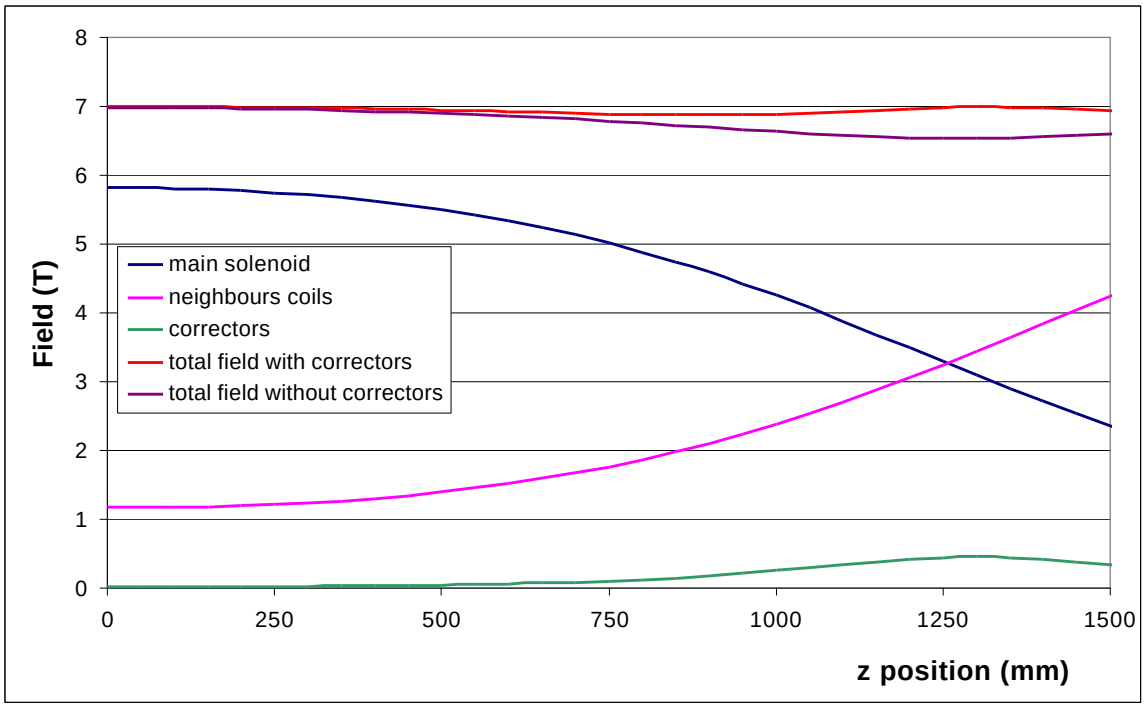

Figure 3-3: on axis high field with and without corrector coils.

3.4.3 – Compensation coils.

Compensation coils may be used in order to limit the field degradation due to the 200mm gaps. These coils are small solenoids having an inner radius of 400mm and a length of 200mm. They leave a sufficient place to install all the cryogenic tubing needed for the liquid hydrogen absorber and for the feeding of the accelerating cavities. They are realized using the conductor of the inner layer of the high field magnet, and adjusting the insulation thickness they provide a current density ranging from 1350 A/mm to 1550 A/mm. The main reason for using this conductor for these magnets is that they have a greater fraction of aluminum than the others, and are therefore less sensitive to the heat deposition coming from the beam. Nevertheless great care should be taken to ensure that the heat deposition that may come from the beam is efficiently evacuated. Their influence on the field homogeneity is shown in figure 3-2 and 3-3. Table 3-6 summarizes the characteristics of these coils.

		Low field corrector	High field corrector
Number of turns		14	16
Conductor	mm x mm	35 x 11.94	35 x 11.94
Inductance	mH	1.14	3.04
Peak field on conductor	T		
Operating point			

Table 3-6: characteristics of the corrector magnets.

3.5 – Quench protection.

3.5.1 – Quench propagation.

The quench propagation velocities in steady state, V_l, can be calculated for each type of conductor using the following formula:

$$V_l = (J / \rho * Cp) * (\rho_e * \lambda / (T_c - T_{op})) ^{½} \qquad (1)$$

Where:

J : mean current density in the conductor after the quench.

ρ : mean density of the conductor.

Cp : average specific heat of the conductor.

ρ_e : electrical resistivity of the conductor.

λ : average thermal conductivity of the conductor.

T_c : critical temperature under the operating field.

T_{op} : operating temperature of the conductor.

The quench velocity is function of the stability margin and the stabilizer content[9].. During the initial stages of the quench the current moves from the superconducting cable and fills progressively the whole section of the aluminum stabilizer[9,10]. The current expelled from the superconducting strands initially affects a small surface and the initial resistance is much greater than the resistance corresponding to the current covering the whole surface of stabilizer. This effect is usually welcome for very big magnets having a low current density in the stabilizer because it eases the identification of the quench, but for the solenoids of the cooling channel it is a drawback. The time constant of the current diffusion inside of the stabilizer can be calculated using:

$$t_m = e_t^2 / (\pi^2 * D_m) \qquad (2)$$

Where:

e_t is the characteristic thickness of the aluminum stabilizer.

$D_m = \rho_e / \mu_0$ magnetic diffusivity.

The transverse quench propagation can also be calculated using:

$$V_t = V_l \quad (\lambda_t / \lambda_l) ^{½} \qquad (3)$$

Where:

λ_l longitudinal conductivity of the conductor.

$\lambda_t = \lambda_i (e_c / e_i)$ transverse conductivity of the winding.

e_c conductor thickness.

e_i insulation thickness.

The time constant for the heat diffusion in the aluminum has the same expression as formula 2, but the magnetic diffusivity D_m is replaced by the Thermal diffusivity D_t, which expression is:

$$D_t = K / \rho * Cp \qquad (4)$$

With K being the thermal conductivity.

These parameters are summarized in table 3-6 for the different conductors.

		Low field and outer layer conductor	High field middle layer conductor	High field inner layer conductor
Longitudinal quench velocity	M/s	67.9	66.1	58.2
Time constant for the current diffusion	milliseconds	14	7	16
Transversal quench velocity	M/s	0.69	0.77	0.87
Time constant for the heat diffusion in the conductor	milliseconds	3.6	3.1	1.9
Current density in the stabilizer after a quench	A/mm2	81.3	66.8	50.1

Table 3-6: conductor parameters related to the quench propagation.

Some comments can be made concerning the data presented in table 3.6. The circumference of the magnet being 5 m, it will take almost the same time for the quench to propagate along the conductor over one turn than for the heat to cross the insulation and propagate the quench axially. The time constant for the heat diffusion in the aluminum stabilizer is between 2 and 8 times faster than the time constant for the current diffusion. Heat generated by the joule effect affects the whole section of the conductor even if the current is localized around the cable.

3.3.2 – Quench detection.

The quench can be detected without doubt once the tension across the magnet has reached a value between 0.5 V and 1V. Table 3-7 summarizes the time needed to reach these values as well as the corresponding temperature of the hot spot and internal resistance of the magnet considering the assumptions presented in paragraph 3.3.4.

		Low field and outer layer conductor	High field middle layer conductor	High field inner layer conductor
Time to reach 0.5V	s	0.5	0.97	1.42
Temperature of the hot spot when 0.5V is reached	K	27	23.2	22.9
Quenched length	m	69	124	172
Time to reach 1V	s	0.87	1.62	2.37
Temperature of the hot spot when 1V is reached	K	30	27.6	27.6
Quenched length	m	118	202	282

Table 3-7: quench data for the different conductors.

3.3.3 – Quench propagators and dump resistor.

Once a quench is detected in a magnet the energy has to be dumped as fast as possible to avoid over heating of the magnet. This is done by increasing the resistance of the magnet, by passing the main current in a diode, and inserting a resistance in series with the magnets. When the current in the magnet will decay, this decay will induce a current in the supporting structure acting as quench back cylinders, contributing to the heat generation and to the propagation of the quench.

The quench heaters used to propagate the quench inside the magnet will be placed at the layer junctions, on the external parts of the solenoids. Once energized these quench heaters will propagate the quench from each end of each layers. Table 3.8 summarize the quench propagation data for each layer considering that only the quench propagation heaters are used to drive the magnet in its resistive state. The mean temperature of the quenched layer is considered as the temperature of the hot spot when half the length of the layer has quenched.

		Low field and outer layer conductor	High field middle layer conductor	High field inner layer conductor
Length of conductor in the layer	m	1780	1316	890
Time to quench one layer	s	13.1	10	7.65
Mean temperature of the quenched layer	K	39.4	32.4	26.2
Mean resistance of the layer	mΩ	2.3	0.73	0.27

Table 3-8: quench propagation data for the different layers of conductor.

An internal dump resistor may be fitted outside the solenoid and consists in a piece of aluminum welded between two points of the conductor and electrically insulated. Between the two welds the aluminum stabilizer of the superconductor is partly removed and a quench heater is glued to it. The quench heater is energized at the same time as the other quench heaters placed at the coil terminations. It leads the superconducting material to its resistive state in a short time, and as the temperature of the conductor increases, the current goes in the aluminum resistance. The respective sections and thermal inertia of the superconducting part and the resistive part are dimensioned in such a way that the most part of the current goes in the resistance. This device is effective to provide an additional resistance to the solenoid during the early stages of the quench.

3.3.4 – Hot spot temperature.

The hot spot temperature has been estimated considering the following hypothesis for the quench propagation and heat exchange:

- The quench propagation occurs at a constant speed for each layer, this speed having the values presented in table 3.6.
- A first heat loss appears due to the longitudinal conductivity of the conductor across a section equal to the aluminum stabilizer cross section. There is no delay considered to start this heat exchange.
- A second heat loss appears due to the conductivity in the electrical insulation. This heat loss is delayed due to the time constant of the heat diffusion across the insulation.
- The current flows into the copper stabilizer within 1ms.
- The current spreads into the aluminum stabilizer within the current diffusion time.
- The initial length of quenched conductor is adjusted to ensure that the energy balance between the heat dissipated by the joule effect and the heat evacuated by conduction does not become negative.

Figure 3-5 shows the temperature rise of the hot spot for each of the conductors. As expected the conductor warm up goes faster for the conductor having less aluminum stabilizer. The dashed lines shows the temperature rise of the conductors of the outer and middle layers if these conductors would not have had copper strands. They heat up much faster because the surface affected by the current diffusion in the early stages of the quench propagation is lower than when the copper wires are present, the resistance being therefore greater. This effect is particularly significant at low temperature because the specific heat of the materials are very low.

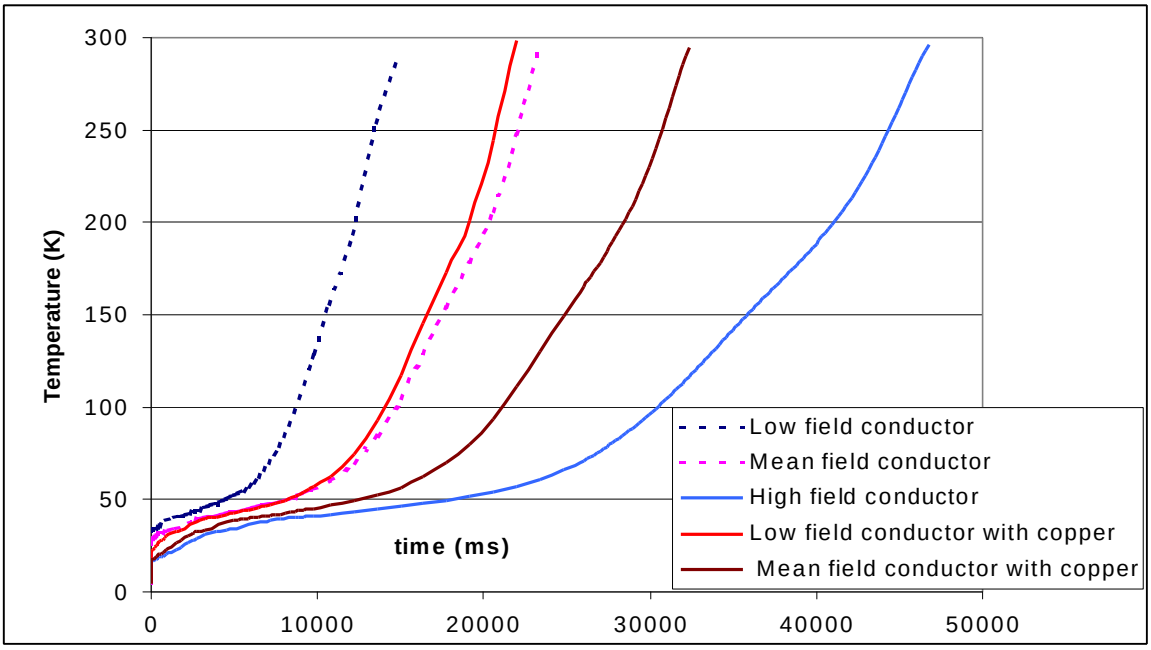

Figure 3-5: heat up of the different conductors during a quench.

3.3.5 – Final mean temperature.

The final mean temperature of the magnets is estimated as if the magnets were made only with aluminum. Table 3-8 gives the values of the final mean temperature of the solenoids if all the energy is dumped in the cold mass.

		Low field magnet	High field magnet
Mass of the cold mass	kg	1950	6850
Stored energy	MJ	18.2	128
Specific stored energy	KJ/kg	9.3	18.7
Final asymptotic temperature if all the energy is dumped in the cold mass	K	80	105

Table 3-8: asymptotic temperature for the magnets after a quench.

4 – Constant field change zone

The constant field change zone sees a field change from –3T to –7T over a length of 53m. 22 main coils are required each of them having a different number of turns. The constant field change magnets are made using the same principles as the high field magnets, except that the innermost winding layer is not fully occupied by conductors. Only the difference from the main solenoids will be described here. Table 4-1 summarizes the properties of the magnets.

Coil number	Mean Field	Number of turns	Number of turns in outer layer	Number of turns in middle layer	Number of turns in inner layer	Inductance
	T					H
12 A	-3	285.4	285			0.0871
12 B	-3.19	304.1	285	19		0.0987
13 A	-3.38	322.9	285	38		0.1111
13 B	-3.57	341.7	285	57		0.1242
14 A	-3.76	360.5	285	75		0.1380
14 B	-3.95	379.3	285	94		0.1525
15 A	-4.14	398.1	285	113		0.1678
15 B	-4.33	416.8	285	132		0.1838
16 A	-4.52	435.6	285	151		0.2005
16 B	-4.71	454.4	285	169		0.2180
17 A	-4.9	473.2	285	188		0.2362
17 B	-5.1	492.0	285	207		0.2551
18 A	-5.29	510.7	285	226		0.2747
18 B	-5.48	529.5	285	227	17	0.2951
19 A	-5.67	548.3	285	227	36	0.3162
19 B	-5.86	567.1	285	227	55	0.3380
20 A	-6.05	585.9	285	227	74	0.3605
20 B	-6.24	604.7	285	227	92	0.3838
21 A	-6.43	623.4	285	227	111	0.4078
21 B	-6.62	642.2	285	227	130	0.4325
22 A	-6.81	661.0	285	227	149	0.4580
22 B	-7	679.8	285	227	168	0.4842

Table 4-1: number of turn per layers and inductance for each of the magnets.

Winding.

Magnets 12A to 18A have only 2 layers for a field change from -3T to -5.5T and magnets 18B to 22B need 3 layers, their field changing from -5.5T to -7T. Spacers are inserted in the winding in order to reduce the mean current density and adjust the field. The width of these spacers reduces as the field increases. Depending of the physics requirement for the field slope, the correction coils (C coils) can be inserted between the main coils to adjust the field variation. The correction coils are similar to the one described in paragraph 3.4.3.

Protection.

Solenoids 12A to 17B are connected in parallel to one diode while solenoids 18A to 22B need one diode per magnet. Each of the magnets has one dump resistor.

5 – Flips zones.

5.1 – First flip

5.1.1 - Magnetic field

At the first flip location the field changes from 3T to –3T over a length of 1.02 m. This location corresponds to cryostat 11. The magnetic field requirement in the region of the first flip is presented in figure 1. The 0 point on the z axis in placed in the middle of the flip, where the magnetic field becomes equal to 0.

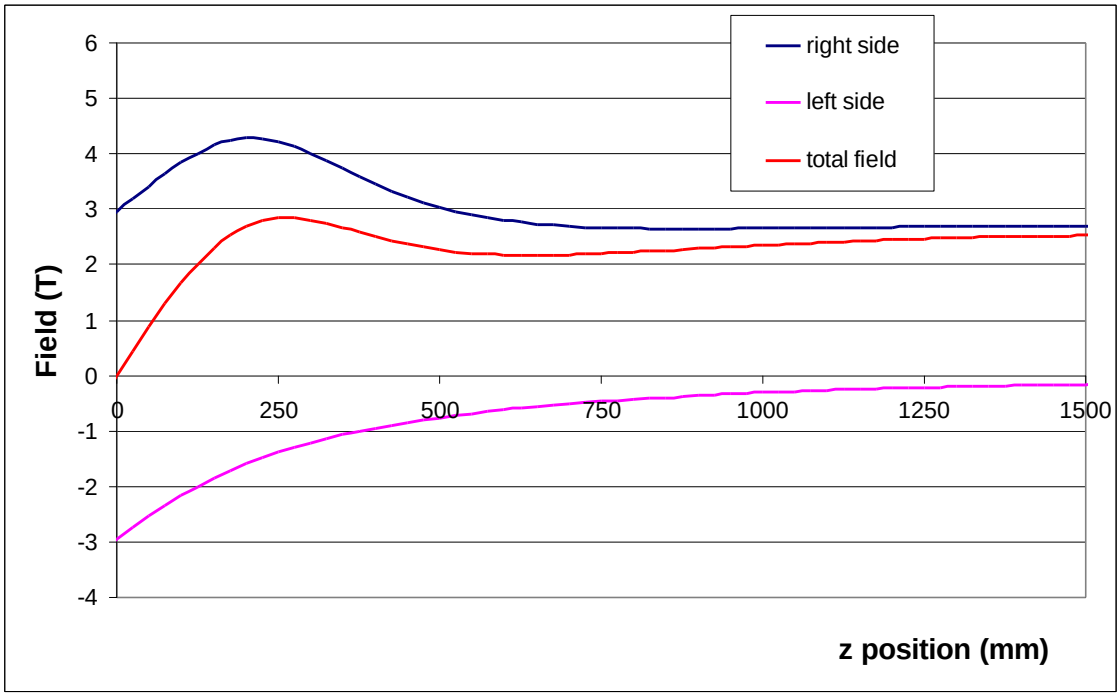

Figure 5-1: field values along the z axis generated by the magnets of the first flip. Only the positive side of the flip is represented, the negative one is symmetrical with respect to z=0.

5.1.2 - Coil parameters

The field inversion is realized using two pairs of magnets, each pair having opposite polarities. The external coils have the same diameters as the main solenoids but are shorter. They are also built on the same principle. The internal coils have an inner bore diameter of 420 mm and a length of 105 mm. The gaps between the coils of the two side of the flip are respectively 200 mm for the outer coils and 268 mm for the inner coils. The characteristics of the set of magnets are presented in table 5-1.

	Outer coil (A and B)	Inner coil (C and D)
Winding pattern	Solenoid	Double pancake
Number of layers	1	22
Coil length	390 mm	105 mm
Winding thickness	35 mm	212 mm
Inner bore radius	800 mm	210 mm
Outer bore radius	988 mm	430 mm
Conductor	7.2 x 35 mm	8.83 x 35 mm
Peak field on conductor	3.15 T	4.55 T

Table 5-1: coil parameters in the first flip.

5.1.3 - Conductor.

The conductor used for the internal coils is the conductor of the middle layer of the main high field solenoids. The peak field on the conductor of the inner coils being 4.55T, the operating point is 0.5 and the temperature margin 2.17K.

At the end of the main coils the operating point increases locally to 0.55 and the temperature margin becomes 2.83K.

5.1.4 - Winding .

The inner radius being too small to allow a longitudinal winding as for the main coils, the winding will be made radially from the middle point (technique called double pancake winding). This technique usually allows only to make a pair number of pancakes. 22 turns are required on each pancake, and 3 pancakes are stacked axially for each of the inner coils. The central double pancake has one pancake in each side of the flip area, the conductor having the same winding direction for both pancakes.

5.1.5 - Insulation.

As for the main solenoids the insulation is made by wrapping one layer of fiberglass ribbon around the conductor at 50% overlap. After completion of the winding, welding of the connections and putting the mechanical structure the coils are vacuum impregnated with epoxy resin.

5.1.6 - Mechanical structure.

The axial forces tend to push away the two half of the flip region from each other. The axial forces are due to the radial field component and increase as the size of the magnet increases. They correspond to the resulting of the magnetic forces integrated on the full circumference and thickness of the conductor winding.

As for the calculation the coils are supposed perfectly aligned the resulting radial force on the different solenoids are equal to 0. The forces on each coil are calculated using the peak field values and presented in table 5-2.

The axial and radial compression in the winding corresponds to the local maximum value of the compression stress that can appear between the coil winding and its supporting structure.

	Axial Forces KN	Axial compression in the winding MPa	Titanium alloy section required to hold the forces (mm^2)
central flip coil (11 C and D)	2633	6.1	5266
outer flip coil (11A and B)	8400	47	16800
outer main coil (10B and 12A)	2320	25	4640

Table 5-2: forces on the different coils, and titanium alloy section required to withhold these forces.

As the outer coils are short, the field change also affects the neighboring magnets (magnets 10B and 12A). These magnets see a radial field component and are subjected to axial forces pushing them away from the flip region. To circumvent this problem, cold tie rods have to be put inside the cryostat number 11 to join the magnets 10B and 12A and hold these forces.

The axial forces between the different coils are high but within the state of the art considering other high loaded magnets. Considering an operating stress of 500 MPa at 4.2K, for titanium alloy[11], the section required to withstand the forces are put in table 5-2. Two solutions to assemble the different solenoids in the cryostat number 11 can be proposed. One solution is to use forged titanium rods to hold the different solenoids together, the other is to have a thick tube between the solenoids of same diameter. Considering the forces seen by the coils 10B and 12A, it is worthwile to use long tie rods going through the cryostat 11 to link both coils together and avoid a highly stressed 300K-4K support. In all the foreseen cases the load transfer between the different solenoids is supposed to be made within the cold part of the structure to limit the size of the parts that will support the thermal gradient (300K/4K).

5.2 – Second flip.

5.2.1 - Magnetic field.

The second flip, located in cryostat 38, is made using the same design as the first one. In this flip the field changes from –7T to 7T over a length of 1.26m. Figure 5-2 shows the on axis field in the flip region.

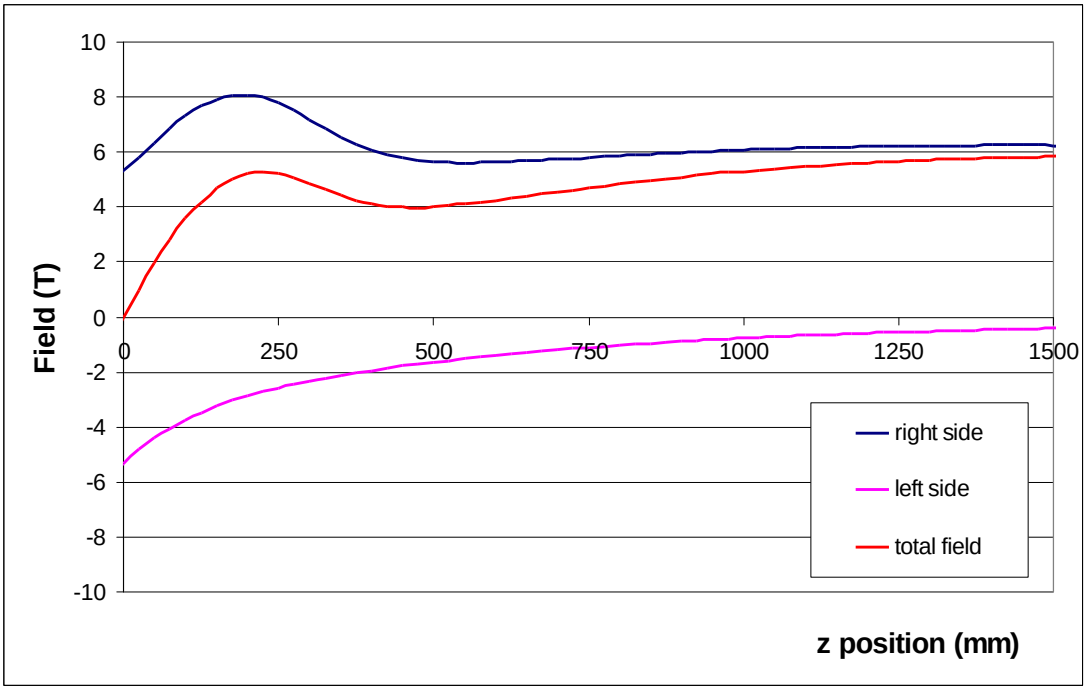

Figure 5-2: field values along the z axis generated by the magnets of the second flip.
Only the positive side of the flip is represented.

5.2.2 - Coil parameters.

The external coils correspond to the coils of the uniform high field zone. The internal coils have an inner bore diameter of 110 mm and a length of 105 mm. The gaps between the coils of the two side of the flip are respectively 200 mm for the outer coils and 96 mm for the inner coils. The characteristics of the set of magnets are presented in table 5-3.

	Outer coil (A and B)	Inner coil (C and D)
Winding pattern	Solenoid	Double pancake
Number of layers	3	10
Coil length	510 mm	245 mm
Winding thickness	105 mm	128 mm
Inner bore	800 mm	110 mm
Conductor	7.2 x 35 mm outer layer 8.83 x 35 mm middle layer 11.94 x 35 mm inner layer	11.94 x 35 mm
Peak field on conductor	6 T	5.8 T

Table 5-3: coil parameters in the second flip.

5.2.3 - Conductor.

The conductor used for the internal coils is the conductor of the inner layer of the main high field solenoids. The peak field on the conductor being 5.8T, the operating point and the temperature margin are respectively 0.39 and 1.74K.

5.2.4 - Winding.

The winding of the inner coils is made as an assembly of double pancakes like the inner coil of the first flip. 10 turns are required on each pancake, and 7 pancakes are stacked axially for each of the inner coils. The central double pancake has one pancake in each side of the flip area, the conductor having the same winding direction for both pancakes.

5.2.5 - Mechanical structure.

The mechanical structure of the second flip has to ensure the same types of constrain than the first one, and the same types of solutions can be used. Table 5-4 summarize the forces between the coils and the longitudinal stresses in the windings.

	Axial Forces KN	Titanium alloy section required to hold the forces (mm^2)	Axial compression in the winding N/mm^2
central coil (Coils 38 C and D)	1726	3452	11
outer coil (Coils 38 A and B)	49470	98940	103
outer main coil (37B and 39A)	29390	58780	52

Table 5-4: forces on the different coils.

The compression in the winding is within acceptable limits for the epoxy based insulation[(12)].

6 – Electrical circuit.

6.1 – General sketch.

The electrical circuit can be subdivided in 3 subelements:

- The magnets, each of them having their protection devices in their cryostats. These items have all been described in chapters 3, 4 and 5.
- The superconducting buses located in the cryogenic lines.
- The room temperature part of the circuit consisting of the main dump resistance, the power supply and the breakers.

The general sketch of the electrical circuit is given in figure 6-1.

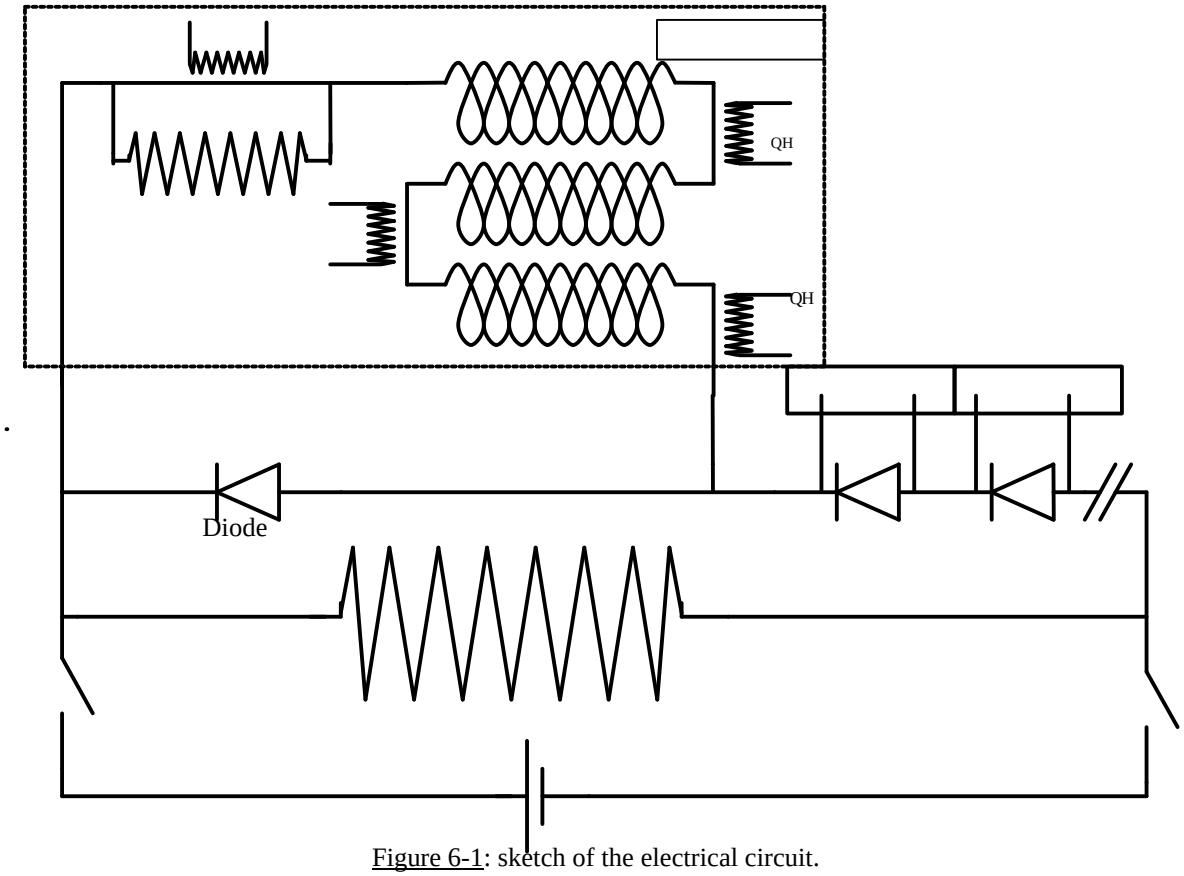

Figure 6-1: sketch of the electrical circuit.

6.2 – Bypass diodes.

Bypass diodes are used to bypass the current in the solenoids that quenches. They are located inside the superconducting bus. These devices have to be developed to support the high current over several minutes.

6.3 – Power supply.

The number of power supplies depends on the time needed to energize the cooling channel. It is foreseen to use 2 power supplies, one located at each end of the channel. The control command system is common for the two power supplies and in the case of a quench in one magnet the whole channel is dumped.

The low field side power supplies will supply the current for the magnets 1A to 30B, respectively 31A to 46A for the high field side power supply. The inductance on each loops are respectively 15.51H and 14.81H .

6.4 – Dump resistors.

The dump resistors have a value of 50 mΩ in order to limit the tension to ground to 1000 V. The time constant for the current decay are respectively 310 and 296 seconds for the low field and high field loops.

6.5 – Breakers.

The breakers are used to remove the power supply from the electrical circuit in the case of a magnet quench. It is assumed that the power supply can be extracted from the circuit in less than 3 seconds once the quench is detected. (ref CMS)

6.6 – Superconducting bus lines.

The bus lines use the high field conductor (35 mm x 11.94 mm) which is oversized with respect to protection and stability problems. The critical current of the conductor and its operating margin in a background field of 1 Tesla are respectively 161 kA and 0.09.

7 – Cryostats and cryogenics.

7.1 – Cryostat

One module of the double flip channel is composed of two cryostats housing two sets of RF cavities and two liquid hydrogen absorbers. 43 modules are considered for the total cooling channel. In order to keep solenoids operating at 4.5 K, we need to shield them from the ambient and from the beam-induced heat loads. Vacuum environment and thermal configurations are important for this purpose.
The cryostat serves to support the solenoid accurately and reliably within the vacuum vessel, to provide all required cryogenic piping, and to insulate the solenoid from heat radiated and conducted from the environment. The heat load due to the conduction in residual gas is dramatically reduced if the vacuum pressure is as low as 10^{-3} Pa. For this reason the vacuum vessel must withstand the vacuum force and will be built out of steel. A 2.4 m long, 2.1 m inner diameter, 12 mm thick vacuum vessel is dimensioned for this application. Titanium bars hooked on the vacuum vessel support the solenoids.

7.2 – Thermal shield and cooling scheme

In this configuration of the cryogenic system, we will consider two cases. One case assumes that the RF cavities are cooled with liquid nitrogen, the other case assumes that the RF cavities operate at room temperature.
The three main temperature levels to consider are the room temperature vacuum vessel, the 4.5 K solenoid and the temperature of the RF cavities. Regarding these large temperature differences, thermal shields are needed to reduce the heat load to the solenoid and to keep it superconducting.

A main actively cooled thermal shield is needed between the vacuum vessel and the solenoid. If liquid nitrogen flowing in a specific circuit cools the RF cavities, then we could use the same circuit in series to cool the thermal shield. The thermal shield is composed of a 3-mm thick aluminum upper shield welded to an extruded lower tray housing the cooling pipe. A gaseous nitrogen mass flow of 15.3 g/s would be necessary to provide a temperature gradient of 1 K over the 2.4-m long thermal shield. The schematic 7-1 illustrates a proposal for the cooling scheme with the case of the high-field magnet powered independently. The pressure drop can be reduced if we choose a large size diameter cooling pipe, therefore the nitrogen pressure can be as low as 3 bar. The real pressure will be determined out of the specification of the RF cavities refrigeration system. Since the RF cavity nitrogen consumption is much larger than the solenoid thermal shield one, the mass flow used for the RF cavity can be partially by-passed.
If no nitrogen circuit is used to cool the RF cavities, gaseous helium flow will assume the refrigeration function as proposed in the figure 7-1.

Brazing cooling pipes to an aluminum foil glued to the solenoid surfaces can materialize a secondary thermal shield named the inner thermal drain. The cooling system of the solenoid is composed of inner thermal drain, which function is to extract the beam-induced heat load, the heat coming from the RF cavities and from the thermal shield described previously. We assume that the supporting system is made out of 0.8 m long Titanium bars hanging the solenoid from the vacuum vessel wall. The total cross-section of Titanium is 5 cm^2 per solenoid. The thermal shield is not in contact with the Titanium bars. If the RF cavities operate at 77 K then the heat load due to conduction and to be extracted by the inner thermal drain is equivalent to approximately 0.9 W over the length of one solenoid. The heat load by radiation from the RF cavities and from the main thermal shield to the solenoid, is equivalent to 1.6 W. Therefore a mass flow of 0.9 g/s of helium flowing in the inner thermal drains at 4.5 K would permit to keep the solenoid at temperature bellow 5 K.

If the RF cavities operate at 300 K, we would need to equip the space in between the RF cavities and the solenoid with an aluminum shield similar to the one between the vacuum vessel and the solenoid. A 3-mm thick aluminum upper shield would be assembled to an extruded lower tray housing the cooling pipe.

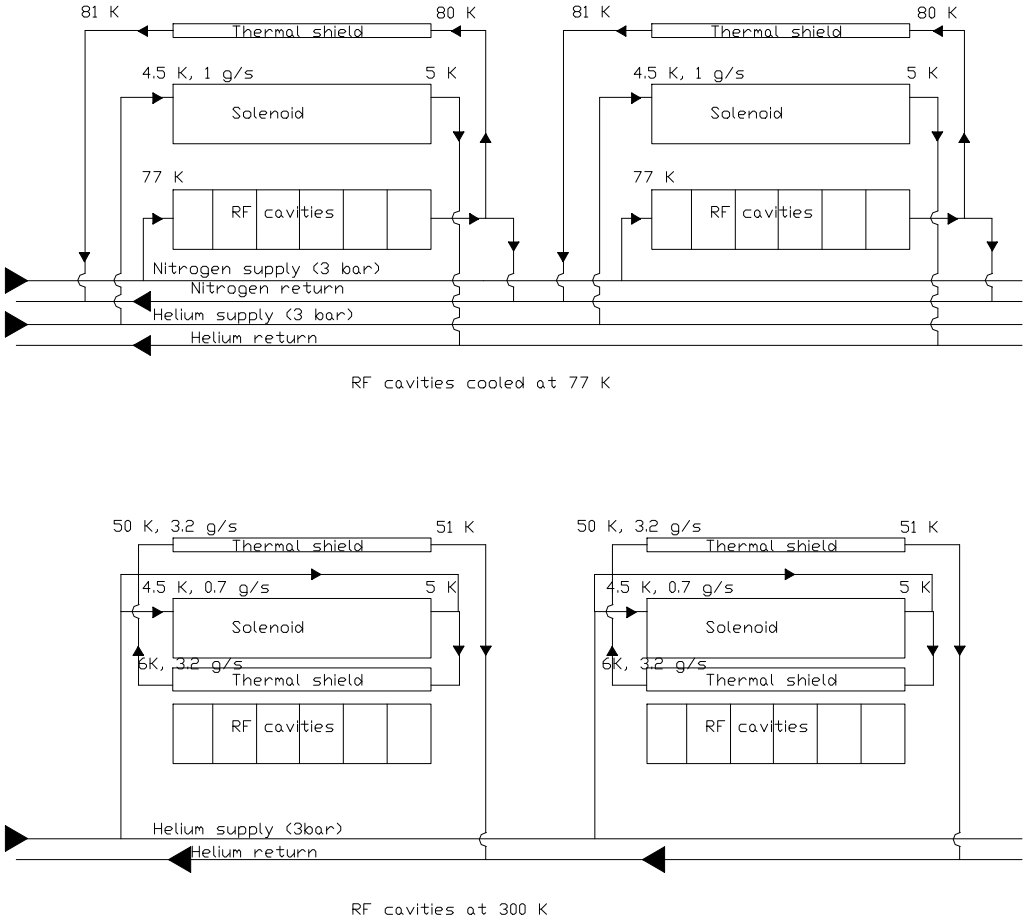

Figure 7-1: cryogenic schematic

7.3 – Superinsulation

The thermal shield is wrapped with superinsulation composed of Multi Layer Insulation (MLI). If we use 30 layers of double side aluminized Mylar foils interleaved with polyester spacers then the heat by radiation from the ambient to the thermal shield is reduced by a factor 24. Therefore, the heat to be extracted by the actively cooled thermal shield is 17 W.
The superinsulation system is only effective to protect the solenoid from the ambient temperature, no superinsulation will be requested to protect the solenoid from the RF cavities temperature at the inner thermal drain temperature level if their operating temperature is 77 K. In the case of the RF cavities operating at room temperature the additional thermal shield in-between the RF cavities and the solenoid also need to be wrapped with MLI in order to reduce to 16.4 W the heat coming from the RF cavities.

7. 4 – Heat loads and cryo-distribution

As introduced in the previous chapters, the distribution of the temperatures and mass-flows determine the heat loads for each temperature level. Figure 7-2 illustrates the heat load distributions to the system for both configurations of RF cavities at 77 K or 300 K.

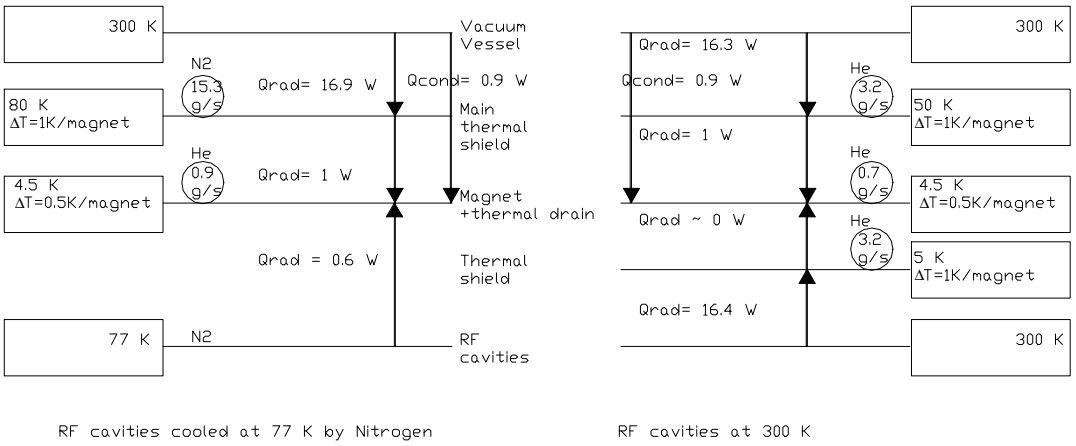

Figure 7-2: heat load distributions for both cases of RF cavity temperatures

The cryo-plant is composed of the nitrogen and the helium circuits if the RF cavities are cooled at 77 K. Helium is used to cool the inner thermal drains. The nitrogen loop is used to cool the RF cavities and the thermal shield. Details of the RF cavity heat loads are not presented here. It is to mention that the RF cavities could also be cooled by gaseous helium, nevertheless this case is not detailed in this chapter.
If the RF cavities operate at 300 K, then the two thermal shields protecting the solenoid and the inner thermal drain will be cooled by helium.
The length of the cryogenic loop needs to be defined regarding the total heat to be extracted from the 43 lattices. The electrical and cryogenics loops installed in parallel will supply each of the 87 solenoids. The cooling loops will couple 2 solenoids in series for the low field magnets and each magnet individually for the high field magnet. The supply and return cryogen lines distribute and collect the different module cooling loops in a parallel network.
If we assume that the RF cavities are cooled by liquid nitrogen, the refrigeration of the total double flip cooling channel can be simplified. The refrigeration by nitrogen will be defined by capacity needed for the RF cavities cooling.

8 – Assembly.

This chapter provides some guidelines for the manufacturing of the magnets, assembly of the submodules and assembly of the full cooling channel.

8.1 – Magnet assembly.

The following operations are required to manufacture the high field magnets:

1. Installing the outer cylinder on the winding machine. A special winding machine dedicated to the solenoids will have to be built.
2. Winding the outer layer.
3. Installing the intermediate cylinder. Thermal shrinkage of the intermediate cylinder can be considered to ease this operation.
4. Winding the middle layer.
5. Installing the inner cylinder.
6. Winding the inner layer.
7. Impregnating the coil with epoxy resin.
8. Gluing the cooling tubes on the external cylinder.
9. Welding the interlayer junctions. The welding of the conductors is made by TIG.
10. Installing the quench propagators and the instrumentation.

8.2 – Subelement assembly.

The following operations are required to assemble the cooling channel subelements:

1. Preparing the central part of the cryostat.
2. Installing and connecting the correction coil in the central part of the cryostat.
3. Installing and connecting the central absorber in the central part of the cryostat.
4. Installing and connecting the accelerating cavities on each side of the central part of the cryostat.
5. Installing and connecting the second absorber.
6. Installing the inner part of the magnets cryostats.
7. Sliding in place the magnets.
8. Connecting the magnets to the central part of the cryostat.
9. Installing the outer part of the magnets cryostats.
10. Sliding in place the external part of the cryostats.

8.3 – Cooling channel assembly.

The following operations are required to assemble the cooling channel in its tunnel:

1. Install the lower cryogenic supply and the bus lines.

The lower cryogenic line contains the electrical busses, including the cold diodes, and the liquid helium inlet pipe and if required the nitrogen inlet pipe.

2. Install the upper cryogenic line.

The upper cryogenic line contains the helium return pipe, the hydrogen cryogenic lines and return gas pipe, and if required the nitrogen return pipe.

3. Put in place the modules.
4. Connect the modules to its neighbors.
5. Connect the modules to the lower cryogenic supply and the bus lines.
6. Connect the modules to the upper cryogenic line.
7. Connect the modules to the instrumentation and to the accelerating cavities power supplies.

9 – Cost estimation.

9.1 – Cost estimation using a size scaling approach.

9.1.1 – Size scaling law.

The size scaling law is based on the scaling laws developed at CERN by A. Herve[13] in 1992 to make the cost estimation of the CMS solenoid. The main parameters involved in the cost of the magnet are the surface of the cryostat, S, and the stored energy, E, in the magnet.

The formulas used for the calculations are the following:

$S = 2 \pi (1.1 \times R) L$ (1) Surface of the cryostat

$V = \pi R^2 L$ (2) Mean magnetized volume

$E = V B^2 / 2 \mu_0$ (3) Stored energy

Where: R is the mean radius of the solenoid
L is the length of the solenoid
B is the central induction in the solenoid
$\mu_0 = 1.257\ 10^{-6}$ H/m

And the formulas for the cost estimation are:

$P_0 = 0.33\ S^{0.8}$ (4) Price of equivalent zero energy magnet in MCHF

$P = P_0 + 0.17\ E^{0.7}$ (5) Price of magnet in MCHF

The coefficients 0.33, 0.8, 0.17 and 0.7 used in the cost estimations have been determined using the experience of the ALEPH cost and the cost estimations made for the CMS solenoid for LHC and the GEM solenoid for SSC. Table 9-1 presents the values used for the determination of the coefficients.

			ALEPH	CMS	GEM
Mean radius of winding	R	m	2.65	3.2	9
Length of vacuum tank	L	m	7	14.5	27
Mean surface of vacuum tank	S	m2	128.2	320.7	1526
Mean magnetized volume	V	m3	154.4	466.5	6870
Central induction	B	T	1.5	4	0.8
Energy	E	MJ	138	2969	1749
P0		MCHF	16.0	33.4	116
P		MCHF	21.4	79.2	147
P0		M$	10.7	22.2	77.3
P		M$	14.3	52.8	98

Table 9-1: cost estimation of the ALEPH, CMS, and GEM solenoids.

Since the cost of the CMS magnet has been reevaluated in 1995 to 84 MCHF, and since the construction has been started within this new price, a coefficient of 1.06 (84/79.2) has been considered to provide an actualized cost.

In order to obtain a price in M$ a change factor of 1 CHF = 0.67 $ has been considered.

9.1.2 –Hypothesis for the calculations.

The power supply, cooling plant, cryostat and cryogenic equipment, vacuum plant are included in this calculation. Of course in the case of the cooling channel if calculations are made for a sum of independent magnets, the result would include the price of one power supply, cryoplant etc.. per magnet and would lead to a substantial overcost. Contingencies, inflation, profit and construction building are not included. This type of calculation allows considering a cost for the magnet even at zero energy.

9.1.3 – Cost estimation.

The cost estimations for the double flip cooling channel presented in table 9-2 are based on the parameters presented in the previous chapters:

The total length of the cooling channel is subdivided in 2 parts, all having an inner cold bore radius of the magnets of 800 mm. It means that the overall cost integrate 2 power supply, cryoplants etc.. The stored energy is calculated separately for each magnet and the total stored energy is calculated for each loop

The flip regions are both considered as if they were equivalent to the mean field in their respective part of the cooling channel. Since the mean field in the flips is 0, the stored energy is lower there.

The actualization coefficient of 1.06 is integrated to the calculation.

			first part	second part	total
Mean radius cryostat	R	m	1.2	1.2	
Length of vacuum tank	L	m	141.5	75.6	217.1
Surface of vacuum tank	S	m2	1174	627	
Mean magnetized volume	V	m3	337	188	
Energy	E	MJ	3740	3668	7408
P0		M$	66.6	40.3	106.9
P		M$	104.7	77.9	182.6

Table 9-2: cost estimations of the different subelements of the double flip cooling channel.

The structure cost, i.e. the cost of making a superconducting magnet of that size independantly of the field produced is 106.9 M$, or 0.49 M$ per meter length. From the second loop, which consist only of 7T magnets, the cost of the high field section is 1.03 M$/m. The corresponding cost of the low field section is 0.54 M$/m, very near the structure cost, which is not surprising since the field is low.

It should be noted that the cost estimation is made as if two long solenoids were made separately. In reality the solenoids will be made as standard sections of 2.4 m long, and one can expect a cost reduction from the batch the production. Typical values of cost reduction in the case of small size industrial production varies from 10 to 25%, depending on the complexity of the items to produce. Therefore a cost reduction between 10 and 20 % can be considered as reasonable, at least for the 3T and 7T constant field magnets. This would lead to an overall cost between 157 M$ and 171 M$ for all the magnets of the cooling channel.

9.1.4 – Factor influencing the cost.

The inner radius of the magnets and the magnetic induction are major cost drivers, and it is therefore interesting to look at their influence on the cost.

Figure 9-1 presents the overall cost as a function of the magnetic field in the high field region. From this figure it comes out that the field dependence is 1.32 M$ per 0.1T.

Figure 9-2 presents the overall cost as a function of the coil inner radius in the whole length of the cooling channel. From this figure it comes out that the radius dependence is 0.3 M$ per centimeter.

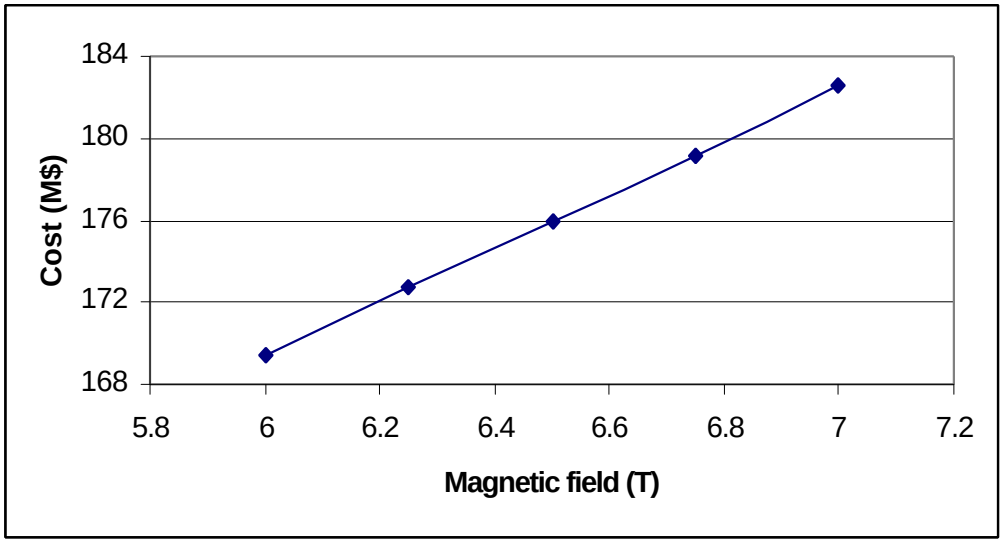

Figure 9-1: overall cost of the cooling channel as a function of the magnetic field in the high field region.

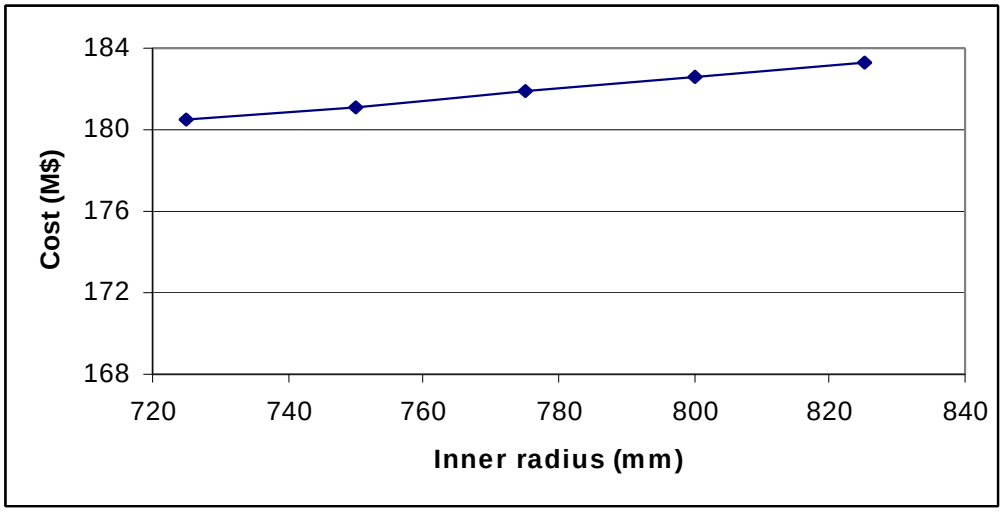

Figure 9-2: overall cost as a function of the coil inner radius of the cooling channel.

9.2 – Cost estimation using a technological approach.

9.2.1 – Superconducting material approach.

Another way to make a cost estimation is to consider a technology to be used to manufacture the magnets, and to scale the price using the cost breakdown from previous magnets. Of course the previous magnets should have used the same technology, and the major cost drivers should be the same.

The estimation is based on the cost of aluminum stabilized conductors. The price of this type of conductor is quite high due to the extrusion of the aluminum stabilizer around the Rutherford cable, and is a major cost driver for the manufacturing of the magnets. In order to be extrapolated the cost of the conductor should be expressed per km of conductor and per kA of critical current at 4.2K. The knowledge of the cost of the ATLAS and CMS conductor, as well as the properties of these conductors allows determining a specific cost of this type of conductors, as shown in table 9-3.

		ATLAS BT	CMS
Cost of conductor	kCHF	14000	18600
Total length of conductor	km	55.36	52
Operating current	kA	20.5	19.5
Critical current	kA	58	56
Operating point		0.35	0.35
Specific cost	kFS/kA.km	4.36	6.39
Specific cost	k$/kA.km	2.91	4.26

Table 9-3: reference costs of the conductors developed for the ATLAS BT and CMS detector magnets.

Some comments should be given concerning the design of the magnets in order to understand the cost difference between these conductors. The ATLAS Barrel Toroid[11] conductor consists of a pure aluminum stabilizer coextruded around a Rutherford cable. The aluminum stabilizer has no mechanical function. In the case of the CMS solenoid[4] the conductor has to contribute to the mechanical structure. In order to do so two mechanical reinforcements made of aluminum alloy are welded on each side of the coextruded pure aluminum stabilizer. The welding operation is made using an electron beam technique. Because of this special technique the cost is significantly higher than for the ATLAS conductor.

9.2.2 – Cost breakdown of large magnets.

The cost breakdown of the CMS magnet is presented in table 4. This cost breakdown does not include the vacuum tank of the cryostat and the iron yoke. The internal cryogenic devices include the thermal screen, the thermosyphon, cryogenic chimneys and the phase separator. The electrical circuit consists of the power supply, the dump resistors, the breakers, the bus bars and the safety and control devices. The external cryogenic devices consist of the cooling plant and his installation. As expected the cost of the superconductor is the major cost driver of the magnet.

Item	Unit cost (MCHF)	fraction
Conductor	19	28%
Winding	16	23%
Assembly	4	6%
Internal cryogenic devices	5	7%
Electrical circuitry	5	7%
External cryogenic devices	8	12%
Surface tests	2	3%
Study and project overview	10	14%
Total cost	69	1

Table 9.4: cost breakdown of the CMS magnet.

9.2.3 – Cost estimation

In order to use the values presented in 3.2 and 3.3 an estimation of the required superconductor is needed to calculate its cost.

Considering a conductor carrying an operating current Iop, at an operating point op, the critical current is expressed at the operating field is expressed as:

$$\mathbf{I}c_{op} = \mathbf{I}_{op} / op \qquad (6)$$

The critical current at the reference point, usually 4.2 K and 5 T for NbTi, is then found as:

$$\mathbf{I}c_{ref} = \mathbf{I}c_{op} * \mathbf{j}c_{ref} / \mathbf{j}c_{op} \qquad (7)$$

Where: $\mathbf{j}c_{ref}$ is the critical current density at the reference point.

$\mathbf{j}c_{op}$ is the critical current density at the operating point.

The values of critical current density as a function of field can easily be calculated using experimental fits[8].

The length of conductor, L, needed to produce the field is:

$$L = \Pi * D * NI / \mathbf{I}_{op} \qquad (8)$$

Where: D is the mean diameter of the coils

NI is the total number of Ampere-turn required to produce the field over the desired length.
Knowing the critical current at the reference point, $\mathbf{I}c_{ref}$, and the required length of conductor, L, the total cost of conductor, C$, can be estimated using the specific cost per km per kA of conductor, c$, as:

$$C\$ = L * \mathbf{I}c_{ref} * c\$ \quad (9)$$

This can also be expressed as:

$$C\$ = (\mathbf{j}c_{ref} / \mathbf{j}c_{op}) \Pi * D * NI / op \quad (10)$$

It should be noted from this last expression that the operating current has no influence on the cost. The magnetic field does not appear directly, but inside the jc factors. As expected since $\mathbf{j}c_{ref}$ is usually taken at 5T, $\mathbf{j}c_{ref} / \mathbf{j}c_{op}$ will be greater than unity for all the magnets producing a field greater than 5T.
The results of the calculations using the parameters of the Cooling Channel are presented in table 9-5.

9.2.4 – Factor influencing the cost.

It can be seen in expression 10 that the operating point, op, has a major influence on the cost. Usually in large detector magnets op is taken between 0.3 and 0.4, and defined for the conductor that withhold the highest field. Therefore the operating point for the outermost layers in the case of a solenoid have an operating point that is much lower. Considering the length of the cooling channel, and the quantity of superconductor needed, the proposed design includes a conductor gradation as a function of the maximum field seen by each layer of conductor.
Table 9-5 presents the estimated cost of the proposed design. As the proposed design uses Nickel reinforced aluminum as stabilizer for the conductors, which is participating to the mechanical structure of the magnets, only the cost of the highly expensive CMS conductor has been considered for the cost estimation.

		Outer layer Conductor	Middle layer Conductor	Inner Layer Conductor
Conductor length	km	147	79	45
Operating current	kA	19.76	19.76	19.76
Field generated	T	3	2.3	1.7
Operating point		0.5	0.54	0.48
Critical current @ 4.2K & 5T	kA	26.4	39.57	70.38
Conductor cost	k$	16532	13317	13492
Total costs				
Total conductor cost	k$	43341	All magnets and conductors together	
Magnets costs	k$	157396		

Table 9-5: cost simulation using different conductors and coil design.

10 – R&D issues.

10.1 – Conductor R&D.

In order to estimate the developments required for the aluminum stabilized conductors it is worthwhile to compare the current density in the winding with the current density of several other superconducting magnets under construction using similar conductor technology. Table 10-1 compares the conductor properties of the muon cooling channel with some of the latest detector magnets under construction.

	current density after a quench (A/mm^2)	Current decay time (s)	Operating point	Peak Field (T)	Stored energy (MJ)	Ref.
Muon cooling channel – Outer layer	81.3		0.5	3	128	
Muon cooling channel – Middle layer	66.8		0.54	5.3	128	
Muon cooling channel – Inner layer	50.1		0.48	7	128	
ATLAS End Cap Toroid	37.5		0.3	4.13	250	7, 14
ATLAS Barrel Toroid	27.2	76	0.3	3.9	1080	5, 11, 14
ATLAS Thin Central Solenoid	53.2		0.25	2.6	39	3, 6, 14
CMS Solenoid	30.4	540	0.4	4.6	2670	4

Table 10-1: comparison between different superconducting magnets, and their superconductor characteristics.

Table 10-1 shows that the conductors proposed for the muon cooling channel all represent a step for one of their characteristics. The inner layer conductor operates locally under high magnetic field, but being stabilized with a lot of aluminum, it has a good stability margin. The outer layer conductor operates at low field and its stability comes from the important temperature rise needed to reach its critical temperature. Once it has quenched, its temperature and resistivity increases faster than for the other layers and this provides the internal resistance required to dump the energy of the magnet. The stability of the different conductors should be measured because the calculations consider the pessimistic case of an operation under their maximum design field. The practical influence of the copper strands should also be measured.

10.2 – Electrical devices.

– Cold diode.

The cold diode used to bypass the current from a quenched magnet is the most challenging device of the double flip cooling channel. Nevertheless the need for such a device is common to several high energy physics large-scale projects, especially the VLHC. Any machine using a 20kA magnet will need such a device, and its development has to be made independently of the need for the cooling channel.

10.3 – Quench simulation.

One other challenge of the proposed magnet design is the quench propagation in the length of the cooling channel. Numerical computations will be required to reduce the loss of energy during a quench and to limit the quench propagation to the lowest number of magnets along the channel.

11 - Conclusion.

Even through tight technical constrains the design of the magnets for the double flip channel is proposed. The field uniformity is satisfactory, as well as the operating margin on the different magnets. The manufacturing techniques are well known from industrial companies producing electrotechnical devices. Some developments are needed during specific R&D operations to finalize the design. The costs are estimated using the production costs of larger magnets currently under construction.

References

1. V. Balbekov, "Double Flip Cooling Channel for Neutrino Factory".
2. S. Geer, "Future Prospects for Muon Facilities", Fermilab – Conf 00/205-E.
3. K. Wada et al., "Development of High Strength and High RRR Aluminium Stabilized Superconductor for the ATLAS Thin Solenoid". IEEE Trans. On Applied Superconductivity, Vol 10, No 1, March 2000. K. Artoos et al., "Status of the Short Dipole Model program for the LHC", IEEE Trans. On Applied Superconductivity, Vol 10, No 1, March 2000.
4. F. Kircher, "Final Design of the CMS Solenoid Cold Mass". IEEE Trans. On Applied Superconductivity, Vol 10, No 1, March 2000..
5. A.Dael et al., "Synthesis of Technological Developments for the B0 Model Coil and the ATLAS Barrel Toroid Coils". IEEE Trans. On Applied Superconductivity, Vol 10, No 1, March 2000.
6. A. Yamamoto et al., "Progress in ATLAS Central Solenoid Magnet". IEEE Trans. On Applied Superconductivity, Vol 10, No 1, March 2000.
7. D.E. Baynham et al.. "Engineering status of the superconducting End Cap Toroid Magnets for the ATLAS Experiment". IEEE Trans. On Applied Superconductivity, Vol 10, No 1, March 2000.
8. Lucca BOTTURA, "A Practical Fit for the Critical Surface of NbTi", IEEE Trans. On Applied Superconductivity, Vol 10, No 1, March 2000.
9. F.P. Juster, et al. 'Stability and Quench Propagation Velocities Measurements on the "Racetrack" Mock-up of the ATLAS Toroid Coil", IEEE Trans. On Applied Superconductivity, Vol 10, No 1, March 2000, p. 677.
10. P. Fabbricatore, et al. "Experimental study of CMS Conductor Stability", IEEE Trans. On Applied Superconductivity, Vol 10, No 1, March 2000, p. 424.
11. ATLAS Barrel Toroid – Technical Design Report – CERN /LHCC/97-19.
12. A. Desirelli, et al. "Finite Element Stress Analysis of the CMS Magnet Coil", ". IEEE Trans. On Applied Superconductivity, Vol 10, No 1, March 2000, p. 419.
13. Alain HERVE – Price of Superconducting Solenoid Magnets, Private Communication, July 1992.
14. H.H.J. ten Kate., "The Superconducting System for the ATLAS Detector at CERN". IEEE Trans. On Applied Superconductivity, Vol 10, No 1, March 2000, p. 347.

Appendix 1: coil and cryostat identification.

Type of area	Cryostat number	Coil number	Mean Field
First cooling – low field	1	A, B and C	3 T
First cooling – low field	2	A, B and C	3 T
First cooling – low field	3	A, B and C	3 T
First cooling – low field	4	A, B and C	3 T
First cooling – low field	5	A, B and C	3 T
First cooling – low field	6	A, B and C	3 T
First cooling – low field	7	A, B and C	3 T
First cooling – low field	8	A, B and C	3 T
First cooling – low field	9	A, B and C	3 T
First cooling – low field	10	A, B, C and D	3 T
First flip	11	A, B and C	
Second cooling – Field change	12	A, B and C	
Second cooling – Field change	13	A, B and C	
Second cooling – Field change	14	A, B and C	
Second cooling – Field change	15	A, B and C	
Second cooling – Field change	16	A, B and C	
Second cooling – Field change	17	A, B and C	
Second cooling – Field change	18	A, B and C	
Second cooling – Field change	19	A, B and C	
Second cooling – Field change	20	A, B and C	
Second cooling – Field change	21	A, B and C	
Second cooling – Field change	22	A, B and C	
Third cooling – High field	23	A, B and C	-7 T
Third cooling – High field	24	A, B and C	-7 T
Third cooling – High field	25	A, B and C	-7 T
Third cooling – High field	26	A, B and C	-7 T
Third cooling – High field	27	A, B and C	-7 T
Third cooling – High field	28	A, B and C	-7 T
Third cooling – High field	29	A, B and C	-7 T
Third cooling – High field	30	A, B and C	-7 T
Third cooling – High field	31	A, B and C	-7 T
Third cooling – High field	32	A, B and C	-7 T
Third cooling – High field	33	A, B and C	-7 T
Third cooling – High field	34	A, B and C	-7 T
Third cooling – High field	35	A, B and C	-7 T
Third cooling – High field	36	A, B and C	-7 T
Third cooling – High field	37	A, B and C	-7 T
Second flip	38	A, ,B C and D	
Fourth cooling – High field	39	A, B and C	7 T
Fourth cooling – High field	40	A, B and C	7 T
Fourth cooling – High field	41	A, B and C	7 T
Fourth cooling – High field	42	A, B and C	7 T
Fourth cooling – High field	43	A, B and C	7 T
Fourth cooling – High field	44	A, B and C	7 T
Fourth cooling – High field	45	A, B and C	7 T
Fourth cooling – High field	46	A, B and C	7 T